Dynamics and particle-hole interactions in liquid ^{3}He: A Green's-function approach

B. E. Clements* and C. W. Greeff†
Department of Physics, University of Delaware, Newark, Delaware 19716

H. R. Glyde
Department of Physics, University of Alberta, Edmonton, Canada T6G 2J1
(Received 10 August 1990; revised manuscript received 11 March 1991)

The dynamics of normal and fully spin-polarized ^{3}He are studied for momentum transfers below 2 Å^{-1}. This study is based on a first-principles calculation of the dynamic susceptibility, $\chi(\mathbf{Q},\omega)$. We invoke the Baym and Kadanoff (BK) procedure for generating an approximate particle-hole irreducible interaction, $I_{\rm ph}$, which is needed in the calculation of $\chi(\mathbf{Q},\omega)$. The BK procedure yields an $I_{\rm ph}$ that conserves particle number, energy, and momentum. When the BK procedure is applied to the Galitskii-Feynman-Hartree-Fock (GFHF) self-energy, the resulting $I_{\rm ph}$ consists of direct and induced terms. Previous calculations using GFHF theory have neglected induced effects. For $Q<2$ Å^{-1}, the induced term contributes significantly to the strength of $I_{\rm ph}$. Landau parameters calculated with induced effects included are greatly improved. We compare our (static) $I_{\rm ph}$ to those obtained from other first-principles calculations, from polarization-potential theories, and from the available experimental data. In spin-polarized ^{3}He, we find that $I_{\rm ph}$ is strongly density dependent. In normal ^{3}He, the same behavior is observed for the spin-symmetric contribution. In contrast, the spin-antisymmetric contribution is nearly independent of density. This finding is in agreement with experiment. For both systems a well-defined zero-sound mode was determined. Using our microscopically determined $I_{\rm ph}$, effective mass, Landau parameter F_1^s, and a polarization-potential form for the frequency dependence of $I_{\rm ph}$, we obtained a zero-sound dispersion that agrees well at low Q with the experimentally determined one. Finally, we comment on the relevance of the spin-fluctuation contribution observed in our $I_{\rm ph}$ for the case of normal ^{3}He.

I. INTRODUCTION

Inelastic neutron-scattering experiments[1] have been highly successful at revealing the properties of the important excitations in liquid ^{3}He. These properties are manifested in the dynamic structure function $S(\mathbf{Q},\omega)$. In a neutron-scattering experiment, both the density and spin-density dynamic structure functions are observed. Denoting the density component by $S_C(\mathbf{Q},\omega)$ and the spin-density part by $S_I(\mathbf{Q},\omega)$, the total observed $S(\mathbf{Q},\omega)$ is given by

$$S(\mathbf{Q},\omega)=S_C(\mathbf{Q},\omega)+\frac{\sigma_I}{\sigma_c}S_I(\mathbf{Q},\omega)\ , \tag{1}$$

where σ_I/σ_c is the ratio of the corresponding scattering cross sections. Q and ω represent the momentum and energy of the density fluctuations created by the scattered neutron. The nature of these excitations depends on the magnitude of the Q and ω probed.[2] In normal ^{3}He, at low Q and ω, one finds a low-frequency (paramagnon) resonance superimposed on the single-pair particle-hole excitations. This resonance, although sharp for small Q ($Q\simeq 0.5$ Å^{-1}), represents a damped nonpropagating mode in the spin density. This damping is expected to be enhanced by incoherent multipair excitations at elevated Q, as has been shown by recently determined sum rules.[3] At higher frequencies a well-defined zero-sound mode (ZSM) in $S_C(\mathbf{Q},\omega)$ is observed. The ZSM is always slightly broadened from overlap with the multipair excitations and is strongly (Landau) damped when it coincides with the particle-hole band.

The neutron-scattering experiments of Scherm *et al.*[4] have produced accurate measurements of $S(\mathbf{Q},\omega)$ for normal ^{3}He for wave vectors in the range $0.3<Q<2.0$ Å^{-1} and for pressures ranging from saturated vapor pressure (SVP) to 2 MPa. Their results include the density dependences of the ZSM and the paramagnon resonance. They find that at low Q the paramagnon resonance is nearly independent of the pressure in contrast to elevated Q ($\simeq 1.3$ Å^{-1}), where $S(\mathbf{Q},\omega)$ shows an increase in intensity with increasing pressure. They also find that the slope of the long-wavelength zero-sound dispersion increases with increasing density. Hess and Pines[5] have used a finite-pressure generalization of the Aldrich and Pines[6] polarization-potential theory to obtain results in good agreement with Scherm *et al.* Although this approach has proven to be a very useful method for studying the dynamics of ^{3}He, its relationship to the many underlying microscopic mechanisms is not always clear. It is one of goals of the present work to use Galitskii-Feynman-Hartree-Fock (GFHF) theory[7–10] to study these phenomena and make this connection.

In the present work we shall focus on investigating the dynamics in systems of normal ^{3}He and fully spin-polarized helium (^{3}He$^\uparrow$). It it not yet possible to produce 100% spin-polarized liquid ^{3}He in the laboratory. Never-

theless, when contrasted to normal ^{3}He, consideration of ^{3}He$^\uparrow$ enables one to assess the importance of spin fluctuations, since these are frozen out in the spin-polarized case. In particular, the term involving S_I in Eq. (1) is absent. There have been many theoretical studies of ^{3}He$^\uparrow$, and of particular relevance to this work is the prediction of a ZSM in this system.[11,12] We will address this issue later in this paper.

Before proceeding, a remark on notation is in order. The following formal development pertains to normal ^{3}He. To recover the results for ^{3}He$^\uparrow$, one need only consider S_C as noted above. In addition, the superscript s which appears on the four-point functions should be understood as referring to all spins up rather than as defined in Eq. (16) below. We use g to denote the number of spin states.

To calculate $S_{C,I}(Q,\omega)$ from standard (Green's function) perturbation theory, it is necessary to introduce the particle-hole irreducible interaction $I_{\rm ph}$. This is achieved by introducing the dynamic susceptibility $\chi_{C,I}(\mathbf{Q},\omega)$:

$$S_{C,I}(\mathbf{Q},\omega)=-\frac{1}{n\pi}\mathrm{Im}\chi_{C,I}(\mathbf{Q},\omega)\ , \tag{2}$$

where $n=N/\Omega$ is the particle number density and $\chi_{C,I}(\mathbf{Q},\omega)$ is given by

$$\chi_{C,I}(\mathbf{Q},\omega)=-\frac{i}{\Omega}\int dt\, e^{i\omega t}\langle T[\rho_\uparrow(\mathbf{Q},t)\pm\rho_\downarrow(\mathbf{Q},t)][\rho_\uparrow^\dagger(\mathbf{Q},0)\pm\rho_\downarrow^\dagger(\mathbf{Q},0)]\rangle\ . \tag{3}$$

In Eq. (2), the $C(I)$ refers to the sum (difference) of the density-fluctuation operators

$$\rho_\sigma^\dagger(\mathbf{Q},t)=\sum_{\mathbf{k}} a_{\mathbf{k}+\mathbf{Q},\sigma}^\dagger(t)a_{\mathbf{k},\sigma}(t)\ . \tag{4}$$

The expectation value is taken with respect to the full interacting ground state. The susceptibility is given by

$$\chi_{C,I}(Q)=\int\frac{d^4p_1\,d^4p_2}{(2\pi)^4(2\pi)^4}\tilde{\chi}_{C,I}(p_1+Q,p_2,p_1,p_2+Q)\ , \tag{5}$$

where the four-point $\tilde{\chi}$ is the solution of the integral equation

$$\tilde{\chi}_{C,I}(p_1+Q,p_2,p_1,p_2+Q)=igG(p_1+Q)G(p_1)\left[(2\pi)^4\delta_{p_1,p_2}-\int\frac{d^4p}{(2\pi)^4}I_{\rm ph}^{s,a}(p_1+Q,p,p_1,p+Q)\tilde{\chi}_{C,I}(p+Q,p_2p,p_2+Q)\right]\ . \tag{6}$$

This is shown diagrammatically in Fig. 1. Formal definitions of (s,a) and the single-particle propagators G are given in the next section. (Note that we have adopted the notation that all vectors are four-vectors unless otherwise specified.) $I_{\rm ph}$ is irreducible in the sense that two separate diagrams, one containing p_1+Q and the other containing $p+Q$, cannot be obtained by cutting a single particle-hole pair in $I_{\rm ph}$.

Aside from the polarization-potential approach[5,6,13] and semiphenomenological approaches based on the induced interaction of Babu and Brown,[14] several first-principles calculations of $I_{\rm ph}$ have been carried out. The relevant calculations pertaining to liquid ^{3}He will be discussed below. However, it should be noted that a similar development has been carried out for the electron gas at metallic densities by Green, Neilson, and Szymański.[15]

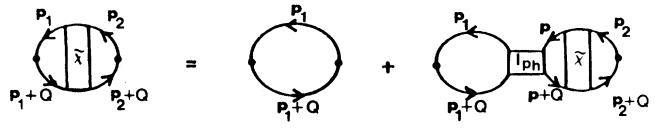

FIG. 1. Diagrammatic representation of $\tilde{\chi}$ in terms of $I_{\rm ph}$. Momenta are four-momenta unless otherwise specified. With the exception of the "legs" of $\tilde{\chi}$, all directed lines are the single-particle propagators $G(\mathbf{k},\omega)$.

Following the work of Glyde and Hernadi,[9] Tanatar, Talbot, and Glyde[10] argued that for intermediate to large momentum transfers ($Q>5.0$ Å^{-1}) $I_{\rm ph}$ can be accurately represented by the GFHF t matrix T. They showed that to a good approximation, for large Q, the t matrix can be reduced to a function of Q and ω alone. The integrations in Eq. (5) are then trivial, and $\chi(\mathbf{Q},\omega)$ reduces to the random-phase-approximation (RPA) expression

$$\chi_{C,I}(Q)=\frac{\chi^0(Q)}{1-I^{s,a}(Q)\chi^0(Q)}\ , \tag{7}$$

where

$$\chi^0(Q)=-gi\int\frac{d^4p}{(2\pi)^4}G(p+Q)G(p)\ . \tag{8}$$

Using this method, they found close agreement with the experimental results of Mook[16] and Sokol *et al.*[17]

At momentum transfers less than several inverse angstroms, the t matrix is not expected to represent accurately $I_{\rm ph}$. From rather general arguments[2] it is known that the low-Q behavior of $I_{\rm ph}^s$ must be repulsive in order

for the system to support a ZSM. However, in this regime the GFHF t matrix is a predominantly attractive interaction. This fact is responsible for the binding of the fluid in the GFHF theory.[7] Further insight is gained by considering the Landau limit. The Landau parameter F_0^s calculated directly from the t matrix was shown to be large and negative.[7,8] However, if one calculates F_0^s from the compressibility using the same approximation to the ground-state energy, the result is positive. This is true for both normal and spin-polarized ^{3}He. An F_0^s calculated from the compressibility includes the effects of varying the interaction with respect to changes in the quasiparticle distribution $n(\mathbf{k})$ about the Fermi surface. This idea is central to the self-energy rearrangement term considered in Refs. 7 and 18. More relevant to the present work, it indicates the importance of including these "polarization" effects in $I_{\rm ph}$.

To determine a suitable form for $I_{\rm ph}$ that includes polarization effects, we have invoked the well-known prescription of Baym and Kadanoff[19,20] (BK). The importance of the BK prescription is that for any approximation to the self-energy, the BK $I_{\rm ph}$ is guaranteed to conserve number, energy, and momentum. The BK prescription is most easily stated in coordinate space:

$$I_{\rm ph}(1,2,3,4)=i\frac{\delta\Sigma(1,3)}{\delta G(4,2)}\ , \tag{9}$$

where $1=(x_1,t_1,\sigma_1)$. In this equation, $\Sigma(1,3)$ and $G(4,2)$ are self-consistently determined. The GFHF self-energy is known to yield a good representation[7-9] of the single-particle properties of ^{3}He, and we choose it for our ansatz for the self-energy. The GFHF self-energy is depicted in Fig. 2 and is expressed in terms of the exchange-symmetrized t matrix T^{sy} as follows:

$$\Sigma(\mathbf{k}_1,\omega_1) = -i\sum_{\sigma_2}\int\frac{d^4k_2}{(2\pi)^4}T^{sy}_{\sigma_1\sigma_2,\sigma_1\sigma_2}(k_1,k_2,k_1,k_2)G(k_2)\ . \tag{10}$$

We have omitted the spin labels since, for an isotropic system, $\Sigma_\uparrow(\mathbf{k},\omega)=\Sigma_\downarrow(\mathbf{k},\omega)$. (In Sec. II we provide a brief review of GFHF theory.)

This choice for the self-energy yields the T approximation discussed quite generally by Baym and Kadanoff[19] and has been used in nuclear matter calculations, for example, by Klemt, Moszkowski, and Speth.[21] The technical details for evaluating $I_{\rm ph}$ [Eq. (9)] with the form (10) for Σ and reducing the result to a numerically tractable form are deferred until Sec. III. The diagrammatic representation of the result is shown in Fig. 3. It consists of two terms. The first term is the t matrix considered in Ref. 10 and follows from cutting the external G line in Fig. 2. As discussed above, this term dominates in the high-Q limit. The second term arises upon differentiating the implicit G dependence of the t matrix. Consequently, it contains polarization effects, as mentioned above. It is obvious from Fig. 3 that the T approximation is the truncation of a complete series of diagrams obtained by replacing one of t matrices in the polarization term with $I_{\rm ph}$, itself. Thus the T approximation to $I_{\rm ph}$ is the second-order approximation to the full solution of the cross-channel Bethe-Salpeter equation considered in the induced interaction models following Babu and Brown.[14] In the present study we shall refer to the second term in $I_{\rm ph}$ as our induced term.

In Sec. IV we use our numerical calculations of $I_{\rm ph}$ to show that the induced term is as important as the direct term in the low-Q limit. In that section we compare our finite-momentum results to the polarization-potential results,[6] correlated basis function results,[11,22] and calculations using the G matrix.[12,23] The density dependence of $I_{\rm ph}$ is presented. Zero-sound-mode dispersion curves are calculated for normal and spin-polarized ^{3}He. In the ZSM calculations we use a model frequency dependence for $I_{\rm ph}$. We then discuss the formal relationship between the Baym-Kadanoff $I_{\rm ph}$ and the Landau parameters. We compare our Landau parameters with those of previous calculations and experiment. The role of spin fluctuations in determining effective-mass enhancement is examined. Finally, in Sec. V we close with a discussion of the shortcomings of this and similar calculations and present directions for future work.

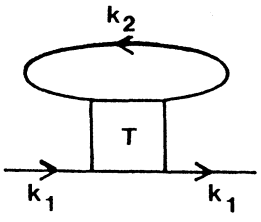

FIG. 2. Diagrammatic representation of the GFHF self-energy.

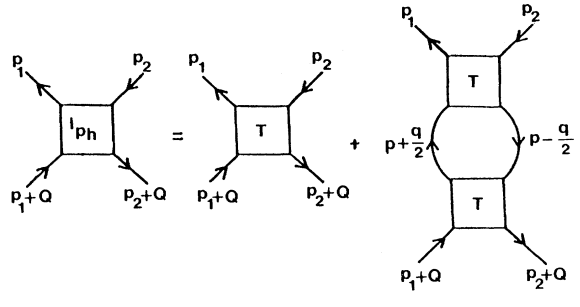

FIG. 3. Diagrammatic representation of the particle-hole irreducible interaction obtained from the GFHF self-energy and the Baym-Kadanoff method. The first and second terms are referred to as the direct and induced terms, respectively.

II. GFHF THEORY

GFHF theory is an extension of Hartree-Fock theory in which the bare interaction $V(r)$ is replaced by the Galitskii-Feynman t matrix T. The corresponding self-energy was already introduced in Sec. I and is shown in Fig. 2. The t matrix, which is obtained by summing the ladder diagrams (Fig. 4), has its primary effect in replacing the hard core of $V(r)$ with a renormalized "soft" core. Analytically, T is obtained by solving the Bethe-Salpeter equation

$$T(k_1,k_2,k_3,k_4)=V(k_1-k_3) + i\int \frac{d^4k_5}{(2\pi)^4} V(k_1-k_5)G(k_5) \times G(k_1+k_2-k_5) \times T(k_5,k_1+k_2-k_5,k_3,k_4) , \tag{11}$$

where $V(k)$ is the Fourier transform of $V(r)$. In the present work $V(r)$ is the HFDHE2 potential of Aziz *et al.*[24] For an instantaneous interaction, T depends on the frequency only through $E=\omega_1+\omega_2$. In contrast to Brueckner G-matrix calculations,[18,23] the t matrix keeps the hole-hole intermediate states.

In Eqs. (10) and (11), the single-particle propagator $G(\mathbf{k},\omega)$ is taken to have the form

$$G(\mathbf{k},\omega)=\frac{1-n(\mathbf{k})}{\omega-\varepsilon(\mathbf{k})+i\eta}+\frac{n(\mathbf{k})}{\omega-\varepsilon(\mathbf{k})-i\eta} . \tag{12}$$

Here $\varepsilon(\mathbf{k})$ and $n(\mathbf{k})$ are the single-particle energy and momentum distribution. In the absence of a magnetic field, $G(\mathbf{k},\omega)$ is diagonal in spin space. Consequently, the spin labels have been suppressed in Eq. (12). This form for $G(\mathbf{k},\omega)$ is based on the quasiparticle picture of a Fermi liquid. In this expression there is the additional assumption that the quasiparticle strength $z_{\mathbf{k}}=[1-\partial\Sigma(\mathbf{k},\omega)/\partial\omega|_{\varepsilon(k)}]^{-1}$ is unity for all k. This is a primary approximation in the GFHF analysis. We note, however, that, unless corrective background terms are added to Eq. (12), it is probably best to satisfy particle-number conservation by setting $z_{\mathbf{k}}$ strictly equal to one.

The calculation of the t matrix requires $\varepsilon(\mathbf{k})$ as input. This is obtained from the (on-shell) GFHF self-energy $\Sigma(\mathbf{k},\varepsilon(\mathbf{k}))$ by the relation

$$\varepsilon(\mathbf{k})=\frac{k^2}{2m}+\mathrm{Re}\,\Sigma(\mathbf{k},\varepsilon(\mathbf{k})) , \tag{13}$$

where m is the bare mass. Equation (13) is simply the assertion that the poles of the single-particle Green's function, as expressed by a Dyson's equation, are the single-particle energies. In turn, the self-energy follows from the t matrix [Eq. (10)], and in this way self-consistency is achieved.

The solution of Eq. (11) yields the "direct" t matrix,

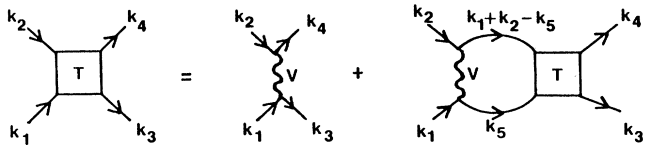

FIG. 4. Bethe-Salpeter equation for the t matrix in the particle-particle channel.

which obeys the spin relation

$$T_{\sigma_1\sigma_2,\sigma_3\sigma_4}(k_1,k_2,k_3,k_4)=T(k_1,k_2,k_3,k_4)\delta_{\sigma_1\sigma_3}\delta_{\sigma_2\sigma_4} . \tag{14}$$

The GFHF self-energy also has a contribution from the exchanged interaction. Consequently, it is useful to introduce an exchange-symmetrized interaction

$$T^{sy}_{\sigma_1\sigma_2,\sigma_3\sigma_4}(k_1,k_2,k_3,k_4)=T(k_1,k_2,k_3,k_4)\delta_{\sigma_1\sigma_3}\delta_{\sigma_2\sigma_4} - T(k_1,k_2,k_4,k_3)\delta_{\sigma_1\sigma_4}\delta_{\sigma_2\sigma_3} . \tag{15}$$

We also define, in analogy with the well-known Landau parameters, the spin-symmetric and antisymmetric interactions

$$T^{s,a}=\tfrac{1}{2}(T^{sy}_{\uparrow\uparrow,\uparrow\uparrow}\pm T^{sy}_{\uparrow\downarrow,\uparrow\downarrow}) . \tag{16}$$

The solution of Eq. (11) is detailed in Ref. 7. Here we note only those features that are important to the present work. Momentum conservation allows T to be expressed as a function of the relative and center-of-mass three-momenta:

$$\mathbf{k}=\tfrac{1}{2}(\mathbf{k}_1-\mathbf{k}_2) , \quad \mathbf{k}'=\tfrac{1}{2}(\mathbf{k}_3-\mathbf{k}_4) , \quad \mathbf{P}=\mathbf{k}_1+\mathbf{k}_2=\mathbf{k}_3+\mathbf{k}_4 , \tag{17}$$

and the total energy E as given above. Following Refs. 7 and 25, we have used an angle-averaged approximation in which the input momentum distributions and energy denominators are averaged with respect to the direction of $\mathbf{P}$. The resulting T depends on P only through its magnitude:

$$T(k_1,k_2,k_3,k_4)\approx T(\mathbf{k},\mathbf{k}',|\mathbf{P}|,E) . \tag{18}$$

Consequently, in the angle-averaged approximation, T depends on k, k', P, E, and $\cos\theta_{\mathbf{k},\mathbf{k}'}$, the direction cosine for k and k'.

Carrying out the spin sum in Eq. (10) replaces T^{sy} with gT^s. Using Eq. (12) and the analytic properties of the t matrix, one obtains the following expression for $\Sigma(\mathbf{k},\omega)$:

$$\mathrm{Re}\Sigma(\mathbf{k}_1,\omega_1)=g\int\frac{d^3k_2}{(2\pi)^3}\left[\mathrm{Re}T^s(\mathbf{k}_1,\mathbf{k}_2,\mathbf{k}_1,\mathbf{k}_2,\omega_1+\varepsilon(\mathbf{k}_2))n(\mathbf{k}_2)-gP\int_{-\infty}^{2\mu}\frac{dE}{\pi}\frac{\mathrm{Im}T^s(\mathbf{k}_1,\mathbf{k}_2,\mathbf{k}_1,\mathbf{k}_2,E)}{\omega_1+\varepsilon(\mathbf{k}_2)-E}\right] , \tag{19}$$

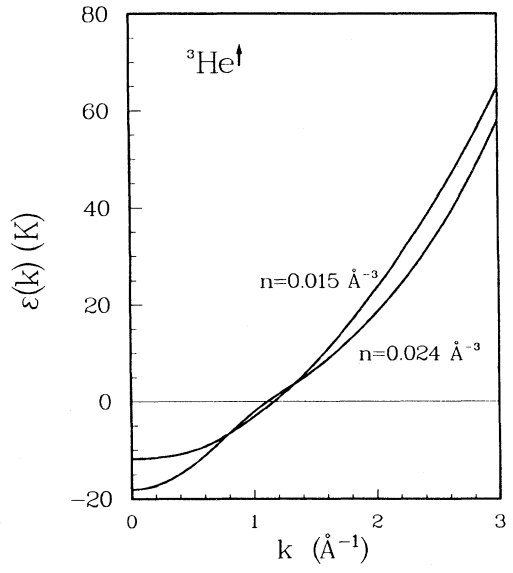

FIG. 5. Single-particle energies for spin-polarized ^{3}He at $n=0.015$ and 0.024 Å^{-3}. These densities correspond to the extreme values of density considered in this work for spin-polarized ^{3}He.

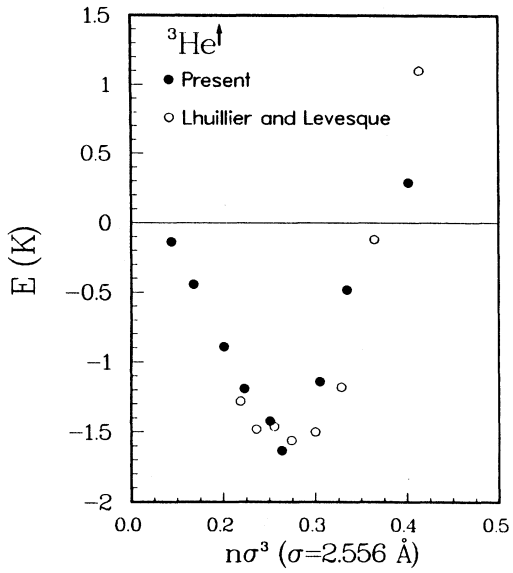

FIG. 6. Density dependence of the binding energy for spin-polarized ^{3}He obtained from GFHF theory (solid circles) and the variational Monte Carlo simulations of Ref. 28 (open circles).

$$\mathrm{Im}\Sigma(\mathbf{k}_1,\omega_1)=g\int\frac{d^3k_2}{(2\pi)^3}\mathrm{Im}T^s(\mathbf{k}_1,\mathbf{k}_2,\mathbf{k}_1,\mathbf{k}_2,\omega_1+\varepsilon(\mathbf{k}_2))[\theta(\mu-\varepsilon(\mathbf{k}_2))-\theta(2\mu-\omega_1-\varepsilon(\mathbf{k}_2))]\ , \tag{20}$$

where μ is the chemical potential. The second term in Eq. (19) arises from the poles of T above the real-frequency axis which come from the two-hole intermediate states. Although this term has been included in the evaluation of the self-energy in nuclear matter,[26] it is neglected in the present work. Recent studies done on spin-polarized deuterium[27] indicate that this term gives a small correction to the single-particle spectrum.

The self-consistent scheme discussed in the Introduction consists of the simultaneous solution of Eqs. (10)–(13). For completeness, we show graphs of several self-consistent spectra (Fig. 5) and a resulting binding-energy curve (Fig. 6) that are the solutions of these equations. We include binding energies obtained by variational Monte Carlo simulations[28] for comparison. It is important to note that the spectra are continuous at the Fermi wave vector. This is not the case in the Brueckner G-matrix calculations. Finally, we note that in practice, the dependence of the t matrix on P has been neglected in the calculation of the self-energy. In the case of ^{3}He↑, this has been accomplished by setting $P=0$. We note however, that in our analysis of the particle-hole irreducible interaction for normal ^{3}He, we found improved results by using an $\varepsilon(k)$ calculated with P set equal to $2k_F$. The iterated ground-state energy is found to be quite independent of P.

III. ANALYSIS OF PARTICLE-HOLE IRREDUCIBLE INTERACTION

In this section we derive an approximate expression for I_{ph}. The diagram shown in Fig. 3 resulted from performing the functional derivatives in Eq. (9), Fourier transforming back into momentum and frequency space, and performing the spin summation. The analytic result is

$$I^{s,a}_{\mathrm{ph}}(p_1+Q,p_2,p_1,p_2+Q)=T^{s,a}(p_1+Q,p_2,p_1,p_2+Q)+i\int\frac{d^4p}{(2\pi)^4}(T^sGGT^s+A^{s,a}T^aGGT^a)\ , \tag{21}$$

where

$$T^\alpha GGT^\alpha\equiv T^\alpha\left[p_1+Q,p-\frac{q}{2},p_2+Q,p+\frac{q}{2}\right]G\left[p+\frac{q}{2}\right]G\left[p-\frac{q}{2}\right]T^\alpha\left[p+\frac{q}{2},p_2,p-\frac{q}{2},p_1\right]\ ,$$

and $A^s=3$ and $A^a=-1$ ($A^{s,a}=0$) for normal (spin-polarized) ^{3}He. We have introduced the vector $\mathbf{q}=\mathbf{p}_1-\mathbf{p}_2$. Strictly, for ^{3}He↑, I^s and T^s are more appropriately labeled by $I_{\uparrow\uparrow,\uparrow\uparrow}$ and $T_{\uparrow\uparrow,\uparrow\uparrow}$.

In principle, Eqs. (5), (6), and (21) are sufficient to determine $\chi(\mathbf{Q},\omega)$. However, if one is interested in collective effects, the entire series in Eq. (6) must be summed. In full, this calculation would be prohibitively complicated. Thus

we resort to introducing approximations that preserve the RPA expression given by Eq. (7). The immediate problem then is to reduce the full momentum dependence of $I_{\rm ph}$ to a function of Q and ω alone. To accomplish this we define a new function $I(\mathbf{Q},\omega)$ as follows. Iterating Eq. (6) and integrating the results as in Eq. (5) yields

$$\chi=\chi^0+\int\int GGI_{\rm ph}GG+\int\int\int GGI_{\rm ph}GGI_{\rm ph}GG+\cdots , \tag{22}$$

where we have suppressed the arguments for convenience. The RPA expression given in Eq. (7) ignores the momentum and energy coupling between the propagators and vertices. In that case, $I_{\rm ph}$ is assumed to be independent of the internal integration variables. Upon carrying out the integrations, each GG pair contributes a χ^0 factor. A procedure that would improve this approximation is to define $I(\mathbf{Q},\omega)$ as

$$\chi(\mathbf{Q},\omega)=\chi^0(\mathbf{Q},\omega)+\chi^0(\mathbf{Q},\omega)I(\mathbf{Q},\omega)\chi^0(\mathbf{Q}\omega)+\chi^0(\mathbf{Q},\omega)I(\mathbf{Q},\omega)\chi^0(\mathbf{Q},\omega)I(\mathbf{Q},\omega)\chi^0(\mathbf{Q}\omega)+\cdots , \tag{23}$$

where (in full)

$$I^{s,a}(\mathbf{Q},\omega)\equiv\frac{g^2}{\chi^0(\mathbf{Q},\omega)^2}\int\frac{d^4p_1}{(2\pi)^4}\int\frac{d^4p_2}{(2\pi)^4}G(p_1)G(p_1+Q)I^{s,a}_{\rm ph}(p_1+Q,p_2,p_1,p_2+Q)G(p_2+Q)G(p_2) . \tag{24}$$

This choice for $I(\mathbf{Q},\omega)$ makes $\chi(\mathbf{Q},\omega)$ exact to first order in $I_{\rm ph}$. Consequently, we regard Eq. (23) as an improved RPA, which we use here. This procedure can obviously be extended to include higher-order corrections. Parenthetically, this scheme is similar to that used by Green, Neilson, and Szymański[15] in their calculation of the proper polarization contribution to χ in the electron-gas problem.

Inserting Eq. (21) into Eq. (24) yields our expression for $I(\mathbf{Q},\omega)$. The corresponding diagram is shown in Fig. 7. We will refer to the first and second terms as the direct and induced terms, respectively.

To evaluate the frequency integrals in $I(Q)$, a further approximation is required. This is due to the complicated frequency dependence of the interaction as defined by Eq. (21). The t matrix is already a complicated function of the total energy E having poles both above and below the real axis. The induced term is even more complicated in that it cannot be reduced to a function of the total energy alone. For this reason, we restrict our microscopic calculation to the limit of zero frequency ($\omega=0$). Later we consider a model form of the interaction to restore the frequency dependence. Our approximation is to neglect the hole-hole intermediate state terms of the t matrix so that the t matrix is analytic above the real axis.

Consider then the frequency integrations in the direct term (Fig. 7). The ω_1 integrations are easily performed by closing a contour in the upper half complex plane. Expressing only the frequency dependence of the t matrix, the p_1 contribution is

$$-i\int\frac{d^4p_1}{(2\pi)^4}G(p_1+Q)G(p_1)T^{s,a}(\omega_{p_1}+\omega_{p_2})$$

$$=\int\frac{d^3p_1}{(2\pi)^3}\frac{n(\mathbf{p}_1+Q)-n(\mathbf{p}_1)}{\varepsilon(\mathbf{p}_1+\mathbf{Q})-\varepsilon(\mathbf{p}_1)}T^{s,a}(\omega_{p_2}+\varepsilon(\mathbf{p}_1+\mathbf{Q}))+\int\frac{d^3p_1}{(2\pi)^3}n(\mathbf{p}_1)\frac{T^{s,a}(\omega_{p_2}+\varepsilon(\mathbf{p}_1+\mathbf{Q}))-T^{s,a}(\omega_{p_2}+\varepsilon(\mathbf{p}_1))}{\varepsilon(\mathbf{p}_1+\mathbf{Q})-\varepsilon(\mathbf{p}_1)} . \tag{25}$$

Each t matrix $T(\mathbf{k},\mathbf{k}',\mathbf{P},\omega)$ in Eq. (25) has a relative incoming ($\mathbf{k}$), outgoing ($\mathbf{k}'$), and center-of-mass ($\mathbf{P}$) momenta given by

$$\mathbf{k}=\tfrac{1}{2}(\mathbf{p}_1-\mathbf{p}_2+\mathbf{Q}),\quad \mathbf{k}'=\tfrac{1}{2}(\mathbf{p}_1-\mathbf{p}_2-\mathbf{Q}),\quad \mathbf{P}=\mathbf{p}_1+\mathbf{p}_2+\mathbf{Q} . \tag{26}$$

Equation (25) can be simplified by using the following observations. First, the frequency argument of the t matrix in the

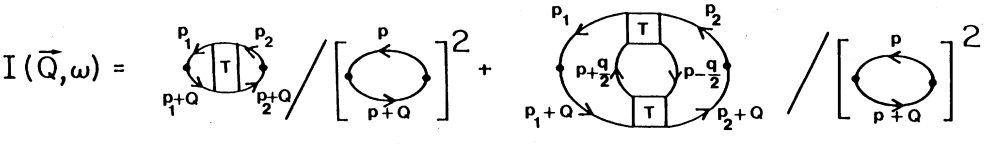

FIG. 7. Our approximation for $I(Q)$ in diagrammatic form.

first term can, to a good approximation, be set equal to $\omega_{p_2}+\varepsilon(k_F)$. This is due to the observation that the susceptibility factor

$$\frac{n(\mathbf{p}_1+\mathbf{Q})-n(\mathbf{p}_1)}{\varepsilon(\mathbf{p}_1+\mathbf{Q})-\varepsilon(\mathbf{p}_1)} \tag{27}$$

is strongly peaked about $|\mathbf{p}_1|=|\mathbf{p}_1+\mathbf{Q}|=k_F$. This fact will be useful when we consider the induced term. Next, we note that because of the known (approximate) linear frequency dependence of the GFHF t matrix, the integrand in the second term is approximately $n(p_1)\partial T/\partial\omega|_{\varepsilon_F}$. Omitting this term is consistent with the approximation of setting $z_{\mathbf{k}}=1$, as discussed in the previous section. Similarly, the ω_{p_2} integrations may be done. The final result for $I_{\rm dir}$ is

$$I^{s,a}_{\rm dir}(\mathbf{Q})=\frac{g^2}{\chi^0(\mathbf{Q},0)^2}\int\frac{d^3p_1}{(2\pi)^3}\int\frac{d^3p_2}{(2\pi)^3}\left[\frac{n(\mathbf{p}_1+Q)-n(\mathbf{p}_1)}{\varepsilon(\mathbf{p}_1+\mathbf{Q})-\varepsilon(\mathbf{p}_1)}\right]T^{s,a}(\mathbf{k},\mathbf{k}',|\mathbf{P}|,2\varepsilon(k_F))\left[\frac{n(\mathbf{p}_2+Q)-n(\mathbf{p}_2)}{\varepsilon(\mathbf{p}_2+\mathbf{Q})-\varepsilon(\mathbf{p}_2)}\right]. \tag{28}$$

$\chi^0(\mathbf{Q},0)$ is the susceptibility given by Eq. (8). In the zero-frequency limit, it reduces to

$$\chi^0(\mathbf{Q},0)=g\int\frac{d^3p}{(2\pi)^3}\left[\frac{n(\mathbf{p}+\mathbf{Q})-n(\mathbf{p})}{\varepsilon(\mathbf{p}+\mathbf{Q})-\varepsilon(\mathbf{p})}\right]. \tag{29}$$

To distinguish this result from the one derived below, we refer to Eq. (28) as our approximation (I) expression for $I_{\rm dir}$.

When considering the induced term, we found it necessary to develop a slightly more restrictive method for reducing the multiple momentum dependences of $I_{\rm ph}$. For clarity and comparison purposes, we first consider the direct term rather than immediately considering the induced term. Our starting point is Eq. (28). Noting once again that the susceptibility factors appearing in Eq. (28) are sharply peaked about

$$|\mathbf{p}_1|=|\mathbf{p}_1+\mathbf{Q}|=|\mathbf{p}_2|=|\mathbf{p}_2+\mathbf{Q}|=k_F \tag{30}$$

implies, that to a good approximation, the t matrix can be factored out of the radial and polar p_1 and p_2 integrations. The legs of T are evaluated at the Fermi surface. A similar observation was made by Pfitzner and Wolfle[29] in their study of the quasiparticle-scattering amplitude. Carrying out the radial and polar integrations yields a $\chi^0(\mathbf{Q},0)^2$ factor, which exactly cancels the denominator. The resulting expression is a function of Q and one remaining angle. A judicious choice for the final angle to integrate over is necessary to ensure the proper Landau limit ($Q\to 0$). Defining a Q-dependent Landau angle as

$$k_F^2\cos\theta_L=(\mathbf{p}_1+\mathbf{Q})\cdot\mathbf{p}_2 \tag{31}$$

will accomplish this. Clearly, as Q goes to zero, this reduces to the usual Landau angle found in the quasiparticle interaction.[7] Our approximation (II) expression for the direct $I(\mathbf{Q})$ is then

$$I^{s,a}_{\rm dir}(\mathbf{Q})=\frac{2}{1-(Q/2k_F)^2}\int_0^{\sqrt{1-(Q/2k_F)^2}}d\left[\cos\frac{\theta_L}{2}\right]\cos\frac{\theta_L}{2}\,T^{s,a}(\tfrac{1}{2}(\mathbf{q}+\mathbf{Q}),\tfrac{1}{2}(\mathbf{q}-\mathbf{Q}),|2\mathbf{b}+\mathbf{Q}|,2\varepsilon(k_F)), \tag{32}$$

where the integration limits and prefactor are a consequence of the restricted phase space imposed by Eq. (30). In Eq. (32) we have introduced the vector $\mathbf{b}=\frac{1}{2}(\mathbf{p}_1+\mathbf{p}_2)$. It is understood that the momenta in these expressions are still restricted by Eq. (30). In the Landau limit the direct term reduces to the expression used in Ref. 7 to evaluate the Landau parameter F_0^s directly from the t matrix:

$$F_0^s=\left.\frac{dn}{d\varepsilon}\right|_{k_F}\int_{-1}^{1}d(\cos\theta_L)T^{s,a}(\cos\theta_L). \tag{33}$$

The density of states at the Fermi surface, $dn/d\varepsilon|_{k_F}$, is introduced to make $F_0^{s,a}$ dimensionless. Obviously, one may obtain the higher-order Landau parameters from Eq. (32) by setting $Q=0$ and integrating over the appropriate Legendre polynomials. It should also be noted that the same $Q=0$ limit can be obtained directly from Eq. (28). This follows immediately by expanding the susceptibility factors [Eq. (27)] about $Q=0$. Consequently, both approximations (I) and (II) are guaranteed to yield the same Landau limit.

We are now in a position to consider the induced term as depicted in Fig. 7. With the assertion that the external momenta be restricted by Eq. (30) and the on-shell prescription, it follows that $\omega_q\approx\varepsilon(p_1)-\varepsilon(p_2)\approx 0$. Thus we can extend the arguments used to arrive at Eq. (32) to justify setting the frequency corresponding to $p\pm q/2$ to $\varepsilon(k_F)$. The resulting induced term is

$$I^{s,a}_{\rm ind}(Q)=\frac{-2}{(1-Q/2k_F)^2}\int_0^{\sqrt{1-(Q/2k_F)^2}}d\left[\cos\frac{\theta_L}{2}\right]\cos\frac{\theta_L}{2}\int\frac{d^3p}{(2\pi)^3}\left[\frac{n(\mathbf{p}+\mathbf{q}/2)-n(\mathbf{p}-\mathbf{q}/2)}{\varepsilon(\mathbf{p}+\mathbf{q}/2)-\varepsilon(\mathbf{p}-\mathbf{q}/2)}\right](T_1^sT_2^s+A^{s,a}T_1^aT_2^a), \tag{34}$$

where

$$T_1^\alpha \equiv T^\alpha(\tfrac{1}{2}(\mathbf{b}-\mathbf{p}+\mathbf{Q}+\mathbf{q}),\tfrac{1}{2}(\mathbf{b}-\mathbf{p}+\mathbf{Q}-\mathbf{q}),|\mathbf{b}+\mathbf{p}+\mathbf{Q}|,2\varepsilon(k_F)) ,$$

$$T_2^\alpha \equiv T^\alpha(\tfrac{1}{2}(\mathbf{b}-\mathbf{p}+\mathbf{q}),\tfrac{1}{2}(\mathbf{b}-\mathbf{p}-\mathbf{q}),|\mathbf{b}+\mathbf{p}|,2\varepsilon(k_F)) .$$

It is understood that the momenta in these expressions are still restricted by Eq. (30). These restrictions allow all the momentum dependences to be written in terms of the integration variables $(p,\cos\theta_p,\phi_p)$, Q, and the Landau angle θ_L. The magnitudes of q and b are, for example, given by the simple expressions

$$|\mathbf{q}| = \left[4k_F^2\sin^2\frac{\theta_L}{2} - Q^2\right]^{1/2}, \quad |\mathbf{b}| = \left[k_F^2\cos^2\frac{\theta_L}{2} + \left[\frac{Q}{2}\right]^2\right]^{1/2} . \tag{35}$$

The upper integration limit in Eq. (34) can be seen to follow from the first of these expressions. The final step needed to evaluate these expressions is to expand the t matrices in a Legendre series:

$$T(\mathbf{k},\mathbf{k}',|P|,E) = \sum_l (2l+1)T_l(|\mathbf{k}|,|\mathbf{k}'|,|P|,E)P_l(\cos\theta_{\mathbf{k}\mathbf{k}'}) . \tag{36}$$

In the next section we compare our $I_{\rm dir}$ calculated from approximations (I) and (II). We argue that this comparison suggests that an $I_{\rm ind}$ determined by Eq. (34), which is based on the assumptions of approximation (II), should be accurate.

IV. RESULTS

We begin this section by presenting the values of the interaction $I(Q)=I_{\rm dir}(Q)+I_{\rm ind}(Q)$, which are the finite-$Q$ solutions of Eqs. (28), (32), and (34). Recall that these equations yield the static ($\omega=0$) irreducible interaction $I(Q)$. We consider spin-polarized ^{3}He first, followed by normal ^{3}He. We close this section with a presentation of Landau parameters, the ZSM, and the role of spin fluctuations in determining effective-mass enhancements.

A. Fully spin-polarized ^{3}He

Figures 8–12 show $I(\mathbf{Q})$ for $^3\mathrm{He}^\uparrow$. Recall that in spin-polarized ^{3}He the spin fluctuations are frozen out and the only interaction is $I_{\uparrow\uparrow,\uparrow\uparrow}(Q)$. Figure (8) shows the direct part of $I(Q)$ given by the t matrix alone [Eqs. (28) and (32)] for the GFHF saturation density $n=0.0172$ Å^{-3}. (The Monte Carlo value of the saturation density is approximately 0.016 Å^{-3}.) Two approximations (I) and (II) given by Eqs. (28) and (32), respectively, used to reduce the momentum dependence of the full $I_{\rm ph}$, are shown. A comparison of the two methods is necessary to test the validity of the more restrictive assumptions used in approximation (II). It is evident from Fig. 8 that the two methods agree well for Q up to $1.7k_F$. It is not surprising that they differ appreciably near $2k_F$. This is a consequence of the restrictions given by Eq. (30). Inspection of these restrictions reveals that approximation (II) can give meaningful results only up to $2k_F$. In fact, as Q approaches $2k_F$, the amount of integrated phase space in approximation (II) quickly drops to zero. For this reason approximation (I) is clearly the more reliable approximation for Q near $2k_F$. Nevertheless, approximation (II) is expected to yield a reliable induced term if one avoids the $2k_F$ regime. In the forthcoming discussion, the direct term is calculated from Eq. (28) and the induced term is calculated from Eq. (34).

In Fig. 9 we illustrate the importance of the induced contribution for finite Q. The dashed line is the direct part of $I(Q)$, and the solid line is the full $I(Q)$. It is clear that the induced contribution has an important role in determining strength of $I(Q)$ for all Q shown. On the

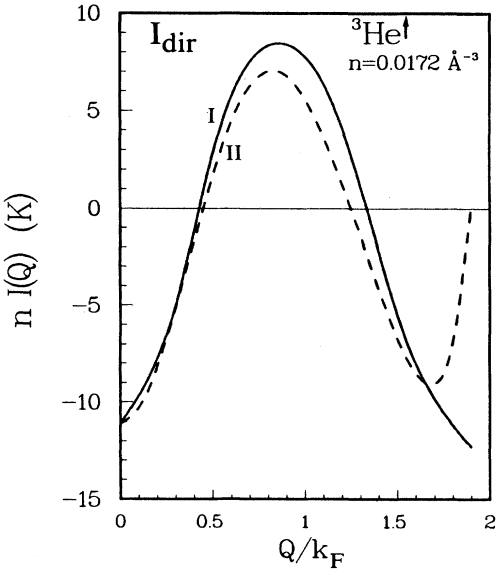

FIG. 8. Two approximations for $I_{\rm dir}(Q)$ in spin-polarized ^{3}He at a density of $n=0.0172$ Å^{-3}. The solid curve (I) is Eq. (28), and the dashed curve (II) is Eq. (32).

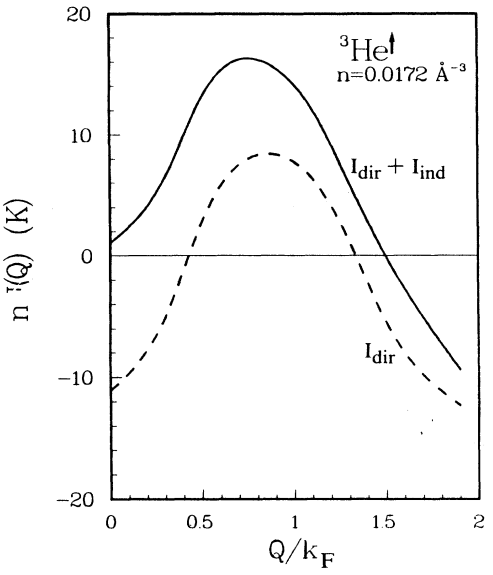

FIG. 9. The direct (dashed curve) and direct + induced (solid curve) terms of $I(\mathbf{Q})$ in ^{3}He$^\uparrow$ as in Fig. 8.

other hand, the direct term largely determines the Q dependence of $I(Q)$.

In Fig. 10 we compare our static $I(Q)$, the correlated basis function (CBF) result of Krotscheck, Clark, and Jackson[11] and the G-matrix calculation of Dickhoff and co-workers.[12,23] The density for all three curves is approximately 0.017 Å^{-3}. Krotscheck, Clark, and Jackson have used CBF theory to calculate a local approximation to $I(Q)$ for normal[22] and spin-polarized[11] ^{3}He. The CBF results compare well with polarization potential results[6] for normal ^{3}He.

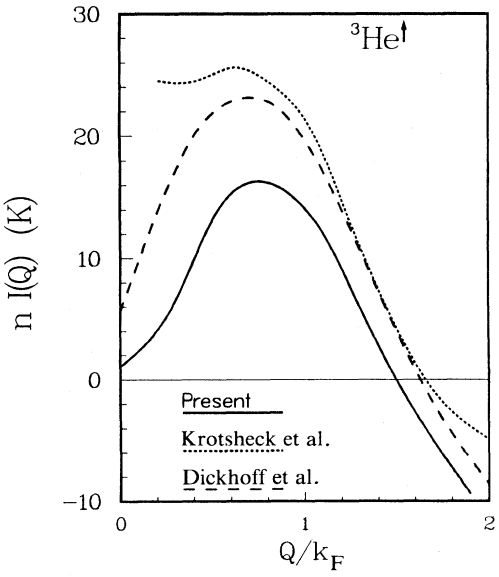

FIG. 10. (Total) $I(\mathbf{Q})$: the present work (solid curve), Krotscheck, Clark, and Jackson (Ref. 11) using CBF theory (dotted curve), and Polls and Dickhoff (Ref. 12) using the G matrix and full cross-channel renormalization (dashed curve). The corresponding densities of ^{3}He$^\uparrow$ are $n=0.0172$, 0.0166, and 0.0169 Å^{-3} for the solid, dotted, and dashed curves, respectively.

In accounting for the substantial difference between our result and the G-matrix results,[12,23] some insight into the importance of a full cross-channel renormalization is gained. This issue is important to the proponents of the many-body parquet formalism. We begin this discussion with a review of the two primary reasons responsible for the observed difference.

First, in the direct term used by Dickhoff and co-workers,[12,23] the effective interaction is the G matrix rather than the GFHF t matrix. For nuclear systems the G matrix is expected to give an accurate representation of the renormalization of the short-range correlations. The G matrix is based on the assumption that the two-hole intermediate states have a negligible role in this renormalization process. Unlike the nucleon-nucleon potential, the ^{3}He-^{3}He potential has a very extended core in position space. This implies that a Fourier representation of the interaction will have important contributions coming from small wave vectors. As a result, the hole-hole intermediate states should not be neglected in ^{3}He. More importantly, however, the GFHF analysis uses a continuous spectrum in contrast to a discontinuous one often used in G-matrix calculations. On iteration, a continuous $\varepsilon(k)$ yields a deeper, more negative direct interaction and a more tightly bound system than does the G matrix for the same density.[7] A consequence of the deeper direct interaction is that the corresponding Landau parameters tend to be substantially more negative than those obtained from a self-consistent calculation involving a spectrum with a gap.[7]

Second, in restricting the set of diagrams that comprise I_{ph} to those prescribed by BK (the T approximation), we have dropped terms beyond second order in T appearing in the cross-channel series. Dickhoff and co-workers[12,23] have made the necessary approximations to sum the entire cross-channel series. By comparing the direct terms calculated from the t and G matrices, we can assess the importance the higher-order terms in the cross channel. In Fig. 10 we display our direct term and one taken from Ref. 12. In the Landau limit, we find that the difference in direct terms is more than sufficient to account for the difference observed in Fig. 10. To a slightly lesser degree, this is also true at finite Q.

We conclude that the primary reason for the difference between our I_{ph} and the one obtained by Dickhoff and co-workers is due to the different choices of spectrums from which the interaction is calculated. This indicates that summing the entire cross-channel series may not be as important in obtaining the gross structure of I_{ph} as summing higher-order self-energy diagrams. Including higher-order self-energy diagrams will have a direct influence on the spectrum. However, the following caveat is important to note. Certain quantities such as I^a for normal ^{3}He are extremely "delicate" and are expected to require the full cross-channel series. This point is discussed below.

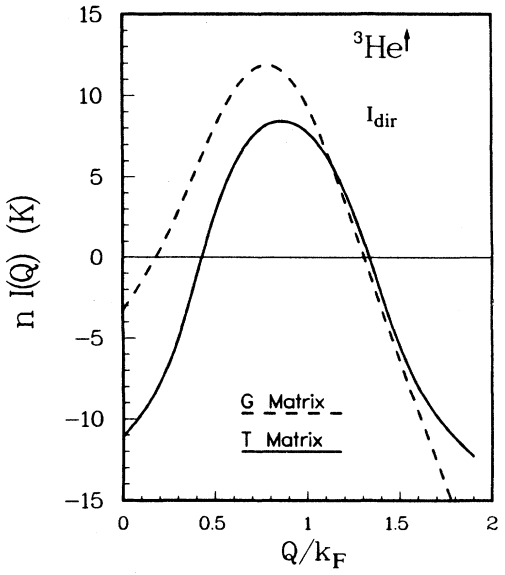

FIG. 11. $I_{dir}(Q)$ from the present work (solid curve) and the G-matrix calculation of Ref. 12 (dashed curve) for $^3He^\uparrow$ as in Fig. 10.

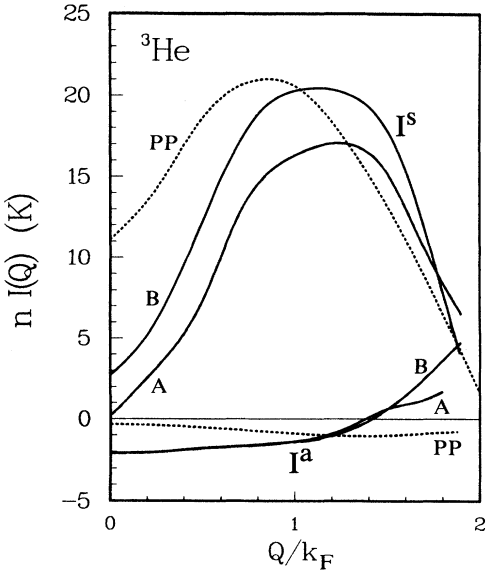

FIG. 13. I^s and I^a for normal ^{3}He at densities of (A) 0.0164 Å^{-3} and (B) 0.0188 Å^{-3}. Also shown is the polarization potentials I^s and I^a from Ref. 6 for $n=0.0164$ Å^{-3} (dotted curve).

The density dependence of $I(Q)$ is displayed in Fig. 12. Of noticeable interest is the rapid increase in the peak strength of I_{ph} with increasing density. This should enhance the possibility of a ZSM being experimentally observed for a sufficiently dense system. The direct part of I_{ph} has a similar, although much weaker, density dependence.

B. Normal ^{3}He

In normal ^{3}He, $I(Q)$ has spin-symmetric (I^s) and spin-antisymmetric (I^a) components. Figure 13 is a plot of the Q dependence of the GFHF I^s and I^a for two values of density, $n=0.0164$ Å^{-3} (SVP) and $n=0.0188$ Å^{-3}. The SVP polarization potentials[6] I^s and I^a are also shown in that figure. Similar to ^{3}He$^\uparrow$, the GFHF t matrix tends to yield an I^s that is smaller than that predicted by other methods.

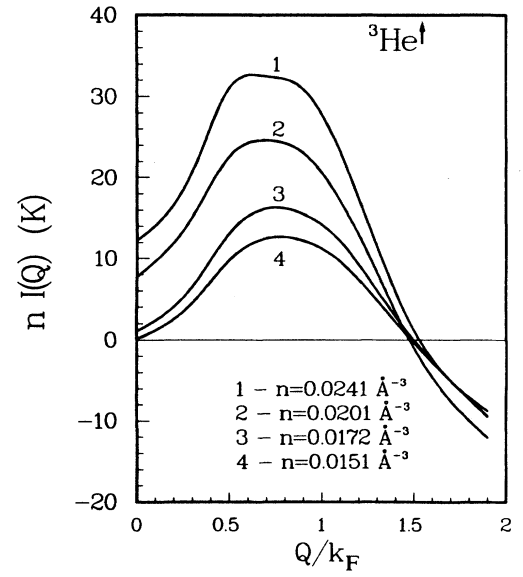

FIG. 12. Density dependence of $I(\mathbf{Q})$ for spin-polarized ^{3}He.

The behavior of I^a shown in Fig. 13 requires some discussion. We begin by noting that our I^a has several characteristics which are desirable. Obviously, our I^a has a qualitative resemblance to the I^a obtained by Aldrich and Pines:[6] The sign of I^a agrees with theirs, and the strength of I^a is an order of magnitude less than that for I^s. Further, in contrast to the strong density dependence of I^s, we find a nearly density-independent I^a. For low Q, this agrees with the experimental findings of Scherm *et al.*,[4] which suggest that the peak portion of the paramagnon resonance changes little with increasing pressure.

Nevertheless, for a Fermi liquid to be stable against a ferromagnetic ordering, it must satisfy $dn/d\varepsilon|_{\varepsilon_F} I^a > -1$. Our I^a violates this condition. Two points should be made in regard to this. First, as emphasized by Aldrich and Pines,[6] an extremely accurate theory is required to obtain an I^a which displays the experimentally observed behavior. More explicitly, they found that the short-range part of $I_{\uparrow\uparrow,\uparrow\uparrow}$ and $I_{\uparrow\downarrow,\uparrow\downarrow}$ (in position space) must differ by less than 3% for the ^{3}He system to be stable against a spin-wave instability. The fact that the GFHF I^a violates this stability condition is not surprising considering the small allowable tolerance. This shortcoming is shared by other purely microscopic calculations[30] which attempt to calculate both ground- and excited-state properties. Second and most important, Quader,

Bedell, and Brown[31] have used the induced-interaction model[14] to show that ferromagnetic ordering cannot occur in a Fermi liquid in the case of a short-range potential. In fact, their proof requires the entire cross channel and χ particle-hole channel to be summed consistently. Since we did not sum the cross channel, our results fail to meet this important criterion.

C. Landau parameters and zero sound

We now present the numerical solutions of Eqs. (28) and (34) in the limit of $Q=0$. These results will be used in the construction of a model for the frequency dependence of $I_{\rm ph}$. We begin with a brief review of the relationship between the Landau quasiparticle interaction $f_{\mathbf{p}_1\mathbf{p}_2}$ and the Baym-Kadanoff $I_{\rm ph}$. The approach of Poggioli and Jackson[32] is the most direct. Starting with the Landau definition of the quasiparticle interaction

$$f_{\mathbf{p}_1\mathbf{p}_2}=\frac{\delta\varepsilon(\mathbf{p}_1)}{\delta n(\mathbf{p}_2)}\ , \tag{37}$$

they have shown that $f_{\mathbf{p}_1\mathbf{p}_2}$ is related to the BK $I_{\rm ph}$ [Eq. (9)] by the integral equation

$$\begin{aligned} f(p_1,p_2,p_1,p_2)=&I_{\rm ph}(p_1,p_2,p_1,p_2)\\ &+i\int\frac{d^4p}{(2\pi)^4}I(p_1,p,p_1,p)\\ &\times G^2(p)f(p,p_2,p,p_2)\ , \end{aligned} \tag{38}$$

where we have been consistent with our previous notation. The relative $(\mathbf{k},\mathbf{k}')$ and center-of-mass $\mathbf{P}$ momenta depend only on the Landau angle through

$$\begin{aligned} |\mathbf{k}|=|\mathbf{k}'|=\tfrac{1}{2}|\mathbf{p}_1-\mathbf{p}_2|=k_F\sin\frac{\theta_L}{2}\ ,\\ |\mathbf{P}|=|\mathbf{p}_1+\mathbf{p}_2|=2k_F\cos\frac{\theta_L}{2}\ . \end{aligned} \tag{39}$$

Before proceeding, we note that Eq. (38) is well known when $I_{\rm ph}$ is exact. Useful discussions have been given, for example, by Nozières[33] and in the nuclear matter problem by Dickhoff *et al.*[34]

The work of Poggioli and Jackson is important to our analysis for a second reason. They have argued that Eq. (38) provides a perturbative scheme for determining f_{p_1,p_2} and that to first order (in their model interaction) f_{p_1,p_2} is simply $I_{\rm ph}$. It should be noted that in their work the use of a restricted (Brandow) space excluded the possibility of a term similar to our induced term from appearing. In the present work we approximate the Landau parameters as the $Q\to 0$ limit of $I_{\rm ph}$.

In Tables I and II, we present our Landau parameters for spin-polarized and normal ^{3}He, respectively. In both cases we list the contributions from the direct term and from the direct plus the induced term. The Landau parameters, obtained from the direct term quoted in earlier references,[7,8] differ from those in Tables I and II because of the fact that in the present work a real input spectrum [Eq. (13)] was used, while in previous work a complex spectrum was used. For comparison, we have included the experimental Landau parameters of Greywall[35] for normal ^{3}He and the Landau parameters determined by the G-matrix calculations of Ref. 23 for ^{3}He$^\uparrow$. The importance of the induced contribution is immediately apparent from these tables. For ^{3}He$^\uparrow$ the F_0 is closer to that predicted by the induced-interaction model of Bedell and Quader.[36] Finally, we note that although the Landau parameters at SVP show significant improvement when induced terms are added, Landau parameters calculated at elevated pressures still differ significantly from those reported by Greywall.

TABLE I. Landau parameters and effective-mass ratios $(=1+F_1/3)$ for spin-polarized ^{3}He. The first and second columns are the Landau parameters calculated from $I_{\rm dir}$ and $I_{\rm dir}+I_{\rm ind}$, respectively. The G-matrix results are taken from Ref. 23. The GFHF and G-matrix values are calculated at densities of 0.0172 Å^{-3} and 0.0169 Å^{-3}, respectively.

	GFHF (direct)	GFHF (total)	G matrix (direct)	G matrix (total)
F_0	−1.36	0.13	−0.30	0.70
F_1	−0.46	−0.97	−1.55	−0.95
m^*/m		0.67		0.68

With $I(Q)$ determined, the ZSM is obtained from the poles of the RPA expression [Eq. (7)] for $\chi_C(Q,\omega)$. We found the imaginary part of $I(Q)$ to be several orders of magnitude smaller than the real part. In this case, the ZSM is undamped when $\mathrm{Im}\chi_0$ is zero. The degree to which the ZSM is pushed up out of the particle-hole band depends, then, on the strength of $I(Q)$ and the effective mass appearing in χ_0. To evaluate χ_0 we used (8), (12), and the GFHF single-particle energies. The GFHF single-particle energies $\varepsilon(p)$ may be well approximated by a quadratic with $m^*/m\approx 0.8$ at the saturation density $n=0.0172$ Å^{-3}. In ^{3}He$^\uparrow$ compressed to $n=0.024$ Å^{-3}, the $\varepsilon(p)$ shows some flattening at $p\approx p_F$ and gives a maximum value of $m^*=p(d\varepsilon/dp)^{-1}$ of $m^*/m=1.2$, just above $p=p_F$.

In Fig. 14 the GFHF ZSM and particle-hole band are shown for ^{3}He$^\uparrow$ for $n=0.0201$ Å^{-3}. The top of the particle-hole band is determined directly from the GFHF self-consistent spectrum. The ZSM is calculated from the static $I(Q)$, alone. The existence of a ZSM in ^{3}He$^\uparrow$ has

TABLE II. Landau parameters and effective-mass ratios $(=1+F_1^s/3)$ for normal ^{3}He. The first and second columns are the Landau parameters calculated from $I_{\rm dir}$ and $I_{\rm dir}+I_{\rm ind}$, respectively. The experimental SVP values are taken from Ref. 35. The GFHF density is 0.0164 Å^{-3}.

	GFHF (direct)	GFHF (total)	Experiment
F_0^s	−9.6	0.20	9.15
F_0^a	−3.5	−1.90	−0.70
F_1^s	1.7	6.3	5.27
F_1^a	−2.7	−0.40	−0.55
m^*/m		3.1	2.76

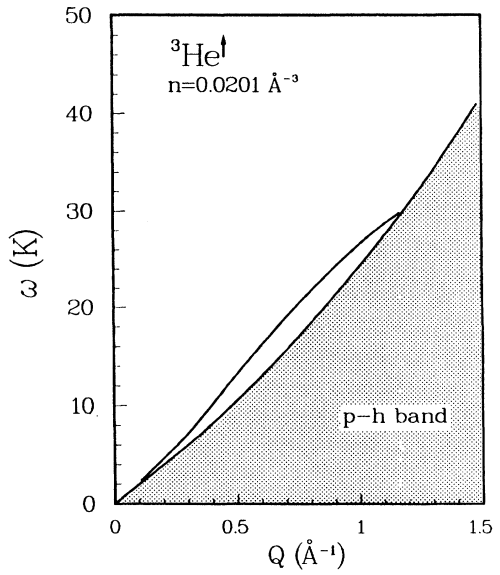

FIG. 14. Zero-sound-mode dispersion curves in spin-polarized ^{3}He at $n=0.0201$ Å^{-3}. This dispersion is calculated directly from the poles of our RPA expression for χ. The corresponding $I(\mathbf{Q})$ is shown in Fig. 12. The frequency dependence of $I(\mathbf{Q})$ has been ignored. Also shown is the top of the GFHF particle-hole band. Use of a frequency-dependent $I(Q)$, as is described in the text for normal ^{3}He, causes the zero-sound mode to merge into the particle-hole band.

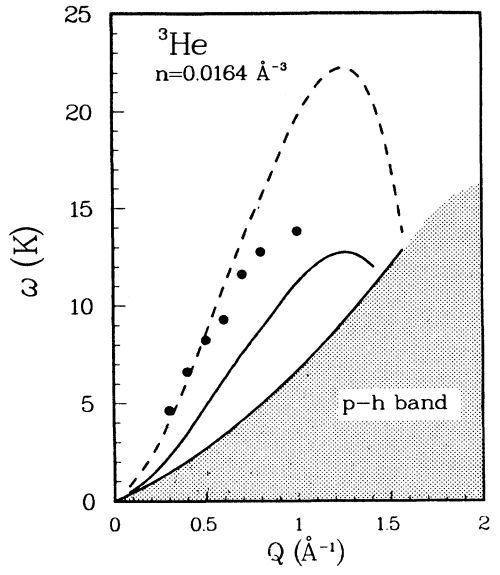

FIG. 15. Zero-sound mode in normal ^{3}He at $n=0.0164$ Å^{-3}. χ_0 and the top of the particle-hole band are determined from a quadratic spectrum where m^* is taken from Table II. Shown in this figure are the zero-sound modes obtained by using $I^s(\mathbf{Q})$ alone (solid curve), by using a frequency-dependent $I^s(\mathbf{Q},\omega)$ as discussed in the text (dashed curve), and the experimental results of Ref. 4 (solid circles).

also been predicted by Krotscheck, Clark, and Jackson[11] and Polls and Dickhoff[12] in the calculations described above.

In normal ^{3}He, a well-defined ZSM is observed.[4] To obtain results which are comparable with experiment, we have calculated χ_0 using single-particle energies of the form $\varepsilon(k)=k^2/2m^*$, with $m^*/m=3.1$, as determined from our F_1^s. The top of the particle-hole band shown in Fig. 15 is obtained from this spectrum. The corresponding $\chi_0(Q,\omega)$ reduces to the well-known Lindhard function with the bare mass replaced by the effective mass. This procedure *violates* the spirit of the Baym-Kadanoff prescription since the self-energies used in the calculation of χ_0 should be the same as those calculated in a self-consistent evaluation of Eq. (10). The need for such an *ad hoc* modification is an indication of the need to include higher-order terms in the self-energy for ^{3}He. The resulting ZSM, obtained from Eq. (7) using our static $I(Q)$, is shown in Fig. 15 as a solid curve. It is important to note that this model for $\chi(Q,\omega)$ does not satisfy the f-sum rule.[2] In polarization-potential theory, for example, one constructs a $\chi(Q,\omega)$ which conserves the f-sum rule by adding a frequency dependent term as follows:

$$\chi_C(Q,\omega)=\frac{\chi_0(Q,\omega)}{1-V^s_{\rm eff}(Q,\omega)\chi_0(Q,\omega)}\ , \tag{40}$$

where

$$V^s_{\rm eff}(Q,\omega)=I^s(Q)+\left[\frac{\omega}{Qv_F}\right]^2\left[\frac{dn}{d\varepsilon}\right]^{-1}\frac{F_1^s}{1+F_1^s/3}\ . \tag{41}$$

In Eq. (41), v_F is the Fermi velocity. This expression is strictly valid for small Q. Obviously, using Eq (41) is still another step removed from the rigorous prescription of the Baym-Kadanoff method where the frequency dependence is exactly defined. Note also that for the sum-rule argument to hold, it is necessary to use in χ_0 an m^*/m which is consistent with F_1^s. In Fig. 15 the dashed curve shows the ZSM obtained from our $I^s(Q)$, which is taken from Fig. 13, and F_1^s, which is taken from Table II. For small Q the agreement with the experimental ZSM is quite satisfactory. One can define a similar frequency-dependent interaction for ^{3}He$^\uparrow$. In this case, F_1 is negative, and the resulting interaction is less repulsive than the frequency-independent one. This decrease in the interaction is sufficient to cause the ZSM to be pushed back into the particle-hole band. Thus, in ^{3}He$^\uparrow$, with $m^*/m\approx 0.7$, a ZSM is unlikely to exist.

D. Role of spin fluctuations

Finally, we close this section with a comment on the role of spin fluctuations in determining $I(Q)$ and the enhancement of the effective mass m^*. Here m^* is given by $m^*/m=1+F_1^s/3$ in Tables I and II with F_1^s obtained from $I=I_{\rm dir}+I_{\rm ind}$. Enhancement of m^* in ^{3}He is generally attributed to spin fluctuations.[30,37–41]

In spin-polarized ^{3}He, where spin fluctuations are frozen out, we obtained $m^*/m=0.7$ at $n=0.0172$ Å^{-3},

in good agreement with previous results.[8,11,23] Thus, in the absence of spin fluctuations, m^*/m is not enhanced above unity. In normal ^{3}He we obtained a mass enhancement to $m^*/m=3.1$, in good agreement with experiment. Using the t matrix alone in I, we obtained $m^*/m=1.5$. Thus most of the enhancement of m^*/m above unity comes from the induced term of I in Eq. (21). The induced term itself contains two terms: T^sGGT^s due to density fluctuations and T^aGGT^a due to spin-density fluctuations. In normal ^{3}He we find that the density-fluctuation term contributes 60% to the induced term, while the spin-fluctuation term contributes 40%. Thus, at the level of our calculation, both density and spin-density fluctuations contribute substantially to the effective-mass enhancement in normal ^{3}He. These results must be interpreted with caution since the T approximation was seen in the previous discussion to yield an I^a which violated the ferromagnetic stability condition. The relation between spin fluctuations and the effective-mass enhancement has most recently been studied by Coffey and Pethick.[41]

In ^{3}He$^\uparrow$, with all spins aligned, the Pauli exclusion principle acts between all pairs of particles. The Fermi repulsion leads to pair correlations which apparently dominate or suppress density fluctuations.[11,28] These pair correlations apparently also reduce density fluctuations or change the character of the T^sGGT^s term of (21) so that m^* is not enhanced by density fluctuations in ^{3}He$^\uparrow$. Indeed, the T^sGGT^s term in ^{3}He$^\uparrow$ reduces m^* somewhat. Thus, not only do spin fluctuations not contribute in ^{3}He$^\uparrow$, but density fluctuations make only a small contribution to m^*. This effect is also observed in electron and nuclear spin-polarized atomic deuterium where $m^*/m<1$ and m^* decreases with increasing density.[27]

Before leaving this topic, we note that Friman and Krotscheck[30] have calculated the ring-diagram contribution to the self-energy for normal ^{3}He. Their calculation uses the local approximation to $I(Q)$ determined in Ref. 22. Similar to us, they also report substantial contributions to the effective mass coming from both the density and spin fluctuations.

V. CONCLUSIONS

We have implemented the Baym and Kadanoff method [Eq. (9)] to obtain the irreducible particle-hole interaction I_{ph} which appears in the dynamic susceptibility. Substituting the GFHF self-energy into Eq. (9), we obtain the T approximation to I_{ph} (depicted in Fig. 3) discussed by BK. This T approximation for I_{ph} is structurally the same as the equation for I_{ph} derived by Babu and Brown. It contains a direct (t matrix) and an induced term: $I_{ph}=I_{dir}+I_{ind}$. In the T approximation, both vertices in the I_{ind} are the t matrix. We have given further approximations which reduce I_{ph} to a function of the momentum transfer Q, only.

Calculations for both normal and spin-polarized ^{3}He show that the characteristic Q dependence of $I_{ph}=I(Q)$ comes from the direct term alone. The induced term gives a nearly constant positive contribution largely independent of Q. In particular, the increase of $I(Q)$ with Q, at low Q, which gives rise to upward dispersion of the ZSM, comes almost entirely from the direct term.

We have also calculated Landau parameters from the interaction I_{ph} and find that the induced term makes an important contribution. Inclusion of the induced term leads to a positive value of F_0^s for both normal and spin-polarized ^{3}He, although our F_0^s for normal ^{3}He is still much smaller than the experimental value. From our F_1^s we calculate an effective mass for normal ^{3}He of 3.1, in quite good agreement with experiment. For ^{3}He$^\uparrow$ we obtain $m^*/m=0.67$, which is consistent with other calculations.[23] In normal ^{3}He we find that the enhancement of m^* to $m^*/m=3.1$ is due to both density and spin-density fluctuations. While our calculations are only approximate, they suggest that density fluctuations are equally important to spin fluctuations in enhancing m^*. Before conclusive statements can be made, one must calculate the entire cross channel (perhaps as was done in Ref. 23) in a method which would have feedback to the spectrum.

Using a model frequency-dependent interaction calculated from our $I(Q)$ and F_1^s in a RPA expression for χ, we calculate a zero-sound mode which agrees well with experiment for normal ^{3}He at low Q. Applying the same model to ^{3}He$^\uparrow$, we find that the frequency-dependent term causes the ZSM to merge into the particle-hole band.

Comparison of the present and other calculations[5,6,22,23] show that qualitatively similar results are obtained from rather different formal approaches. It is therefore tempting to conclude that the dynamics of ^{3}He, at low-momentum transfers, is well understood. Although much has been learned from these studies, it is important to keep in mind that they all share similar shortcomings. The approximations used in the present work are strongly motivated by the need to reduce $\chi(\mathbf{Q},\omega)$ to a RPA form. This is due to the technical complexity of a full solution of Eqs. (5) and (6) including the full momentum and frequency dependences of I_{ph}. However, in reducing I_{ph} to a local, static function, much interesting physical information is lost. For example, the use of a real interaction in Eq. (40) precludes the possibility of damping of the ZSM, which is known experimentally to be substantial. One advantage of the Green's-function approach is that all these effects are, in principle, included. It would therefore be desirable to come up with a scheme which maintains this information to some degree. One possibility, inspired by the work of Green, Neilson, and Szymański,[15] would be to absorb the nonlocal part of I_{ph} into a "screened" χ, where it might be treated perturbatively. This approach has the advantage of maintaining the simple RPA structure for χ while keeping some of the more realistic properties of I_{ph}.

ACKNOWLEDGMENTS

Support from the U.S. Department of Energy, Office of Basic Energy Sciences, under Contract No. DE-FG02-84ER45082, from the National Science Foundation under Contract No. PHY-8806265, and from Texas Advanced Research Program under Grant No. 010366-012 are gratefully acknowledged.

*Present address: Center for Theoretical Physics, Texas A&M University, College Station, TX 77843.
†Present address: Department of Physics, University of Alberta, Edmonton, AB, T6G 2J1.

[1]H. R. Glyde and E. C. Svensson, in *Methods of Experimental Physcis,* edited by D. L. Price and K. Sköld (Academic, New York, 1987), Vol. 23, Chap. 13, p. 303.
[2]D. Pines and P. Nozières, *Theory of Quantum Liquids* (Benjamin, New York, 1966), Vol. 1.
[3]F. Dalfovo and S. Stringari, Phys. Rev. Lett. **63**, 532 (1989).
[4]R. Scherm, K. Guckelsberger, B. Fak, K. Sköld, A. Dianoux, H. Godfrin, and W. G. Stirling, Phys. Rev. Lett. **59**, 217 (1987).
[5]D. W. Hess and D. Pines, J. Low Temp. Phys. **72**, 247 (1988).
[6]C. H. Aldrich III and D. Pines, J. Low. Temp. Phys. **32**, 689 (1978).
[7]H. R. Glyde and S. I. Hernadi, Phys. Rev. B **28**, 141 (1983).
[8]H. R. Glyde and S. I. Hernadi, Phys. Rev. B **29**, 3873 (1984).
[9]H. R. Glyde and S. I. Hernadi, Phys. Rev. B **29**, 4926 (1984).
[10]B. Tanatar, E. F. Talbot, and H. R. Glyde, Phys. Rev. B **36**, 8376 (1987).
[11]E. Krotscheck, J. W. Clark, and A. D. Jackson, Phys. Rev. B **28**, 5088 (1983).
[12]A. Polls and W. H. Dickhoff, in *Spin Polarized Quantum Systems,* edited by I. S. I.-S. Stringari (World Scientific, Singapore, 1989), p. 109.
[13]H. R. Glyde and F. C. Khanna, Can. J. Phys. **55**, 1906 (1977); Phys. Rev. Lett. **37**, 1962 (1976); Can. J. Phys. **58**, 343 (1980).
[14]S. Babu and G. E. Brown, Ann. Phys. (N.Y.) **78**, 1 (1973); T. L. Ainsworth, K. S. Bedell, G. E. Brown, and K. F. Quader, J. Low Temp. Phys. **50**, 319 (1983).
[15]F. Green, D. Neilson, and J. Szymański, Phys. Rev. **31**, 2779 (1985); **31**, 2796 (1985).
[16]H. A. Mook, Phys. Rev. Lett. **55**, 2452 (1985).
[17]P. E. Sokol, K. Sköld, D. L. Price, and R. Kleb, Phys. Rev. Lett. **54**, 909 (1985).
[18]K. A. Brueckner and D. T. Goldman, Phys. Rev. **116**, 1023 (1963). K. A. Brueckner, J. L. Gammel, and J. T. Kabis, *ibid.* **118**, 1438 (1960).
[19]G. Baym and L. P. Kadanoff, Phys. Rev. **124**, 287 (1961).
[20]G. Baym, Phys. Rev. **127**, 1391 (1962).
[21]V. Klemt, S. A. Moszkowski, and J. Speth, Phys. Rev. C **14**, 302 (1976).
[22]E. Krotscheck, Phys. Rev. A **26**, 3536 (1982).
[23]W. H. Dickhoff, H. Müther, and A. Polls, Phys. Rev. B **36**, 5138 (1987).
[24]R. A. Aziz, V. P. S. Nain, J. C. Carly, W. L. Taylor, and G. T. McConville, J. Chem. Phys. **70**, 4330 (1979).
[25]R. F. Bishop, H. B. Ghassib, and M. R. Strayer, Phys. Rev. A **13**, 1570 (1976).
[26]A. Ramos, A. Polls, and W. H. Dickhoff, Nucl. Phys. **A503**, 1 (1989).
[27]C. W. Greeff, B. E. Clements, E. F. Talbot, and H. R. Glyde, Phys. Rev. B **43**, 7595 (1991).
[28]C. Lhuillier and D. Levesque, Phys. Rev. B **23**, 2203 (1981).
[29]M. Pfitzner and P. Wolfle, Phys. Rev. B **35**, 4699 (1987).
[30]B. L. Friman and E. Krotscheck, Phys. Rev. Lett. **49**, 1705 (1982).
[31]K. F. Quader, K. S. Bedell, and G. E. Brown, Phys. Rev. B **36**, 156 (1987).
[32]R. S. Poggioli and A. D. Jackson, Phys. Rev. C **14**, 311 (1976).
[33]P. Nozières, *Theory of Interacting Fermi Systems* (Benjamin, New York, 1964).
[34]W. H. Dickhoff, A. Faessler, J. Meyer-Ter-Vehn, and H. Müther, Nucl. Phys. **A368**, 445 (1981).
[35]D. Greywall, Phys. Rev. B **27**, 2747 (1983).
[36]K. S. Bedell and K. F. Quader, Phys. Lett. **96A**, 91 (1983).
[37]S. Doniach and S. Engelsberg, Phys. Rev. Lett. **17**, 750 (1966).
[38]N. F. Berk and J. R. Schrieffer, Phys. Rev. Lett. **17**, 433 (1966).
[39]G. E. Brown, C. J. Pethick, and Ali Zaringhalam, J. Low Temp. Phys. **48**, 349 (1982).
[40]P. C. E. Stamp, J. Phys. F **15**, 1829 (1985).
[41]D. Coffey and C. J. Pethick, Phys. Rev. B **37**, 1647 (1988).